Journal of Alloys and Compounds 489 (2010) 475–481

Contents lists available at ScienceDirect

Journal of Alloys and Compounds

journal homepage: www.elsevier.com/locate/jallcom

Texture evolution and mechanical properties of AZ31B magnesium alloy sheets processed by repeated unidirectional bending

Bo Song[a,b], Guangsheng Huang[a,b,*], Hongcheng Li[a,b], Lei Zhang[a,b], Guangjie Huang[a,b], Fusheng Pan[a,b]

[a] National Engineering Research Centre for Magnesium Alloys, Chongqing University, Chongqing 400044, PR China
[b] College of Materials Science and Engineering, Chongqing University, Chongqing 400045, PR China

ARTICLE INFO

Article history:
Received 9 August 2009
Received in revised form
15 September 2009
Accepted 16 September 2009
Available online 25 September 2009

Keywords:
Magnesium alloy
Unidirectional bending
Texture
Mechanical properties
Annealing

ABSTRACT

Commercial AZ31B magnesium alloy sheets have poor plasticity and stamping formability at room temperature owing to strong basal texture. In this study, a method termed 'repeated unidirectional bending' (RUB) was applied to improve the mechanical properties of magnesium alloy sheets by controlling the texture. The evolution of the texture and mechanical properties of the sheets during RUB and annealing were systematically investigated. In the sheets that underwent RUB, the *c*-axis tended to become inclined from the normal direction (ND) towards the rolling direction (RD), and the $\{1\,0\,\bar{1}\,2\}$ extension twinning was activated during bending. When a sheet that had undergone RUB was annealed at 260 °C, the mechanical ductility at room temperature was improved considerably because the texture components became more dispersed along the RD, and work hardening was also eliminated by annealing.

1. Introduction

In recent years, magnesium alloys have received great attention in the aviation, automobile and electronics industries because of their low density, high specific strength and ability to be recycled [1]. However, the processing of magnesium and its alloys is relatively difficult at ambient temperature due to their limited ductility, which is essentially attributed to the limited number of slip systems owing to the hexagonal crystal structure. The non-basal slip is hardly operative at low temperatures because critical resolved shear stress (CRSS) of a basal slip system is approximately 1/100 compare to those of the non-basal slip systems on prismatic and pyramidal planes at room temperature [2]. It is now well known that the formation of basal texture away from the rolling plane as well as a decrease in grain size can increase the formability of magnesium [3]. The results indicate that grains were effectively refined by the equal-channel angular extrusion (ECAE) [4–6], cyclic extrusion and compression (CEC) [7–9] and accumulative roll bonding (ARB) [10,11]. The ECAE processes have been known to produce texture with a strong basal component located at 45° between extrusion direction (ED) and ND. However, in the conventional sense, it is only applicable for rod products. The application base, however, is more extended for flat products, which essentially require the rolling behavior to be improved. However conventional rolling generally gives rise to a strong basal texture in magnesium alloy sheets [12,13], i.e. *c*-axis perpendicular to the rolling plane, which increases the difficulty in deformation accompanying with thickness reduction and leads to a very limited formability near the room temperature. At present, the asymmetric rolling (ASR) was used to process the magnesium alloy sheet with rotating the basal plane away from the rolling plane. Several investigations into the microstructure of and texture evolution in magnesium alloys processed by asymmetric rolling can be found in the literature [12,14–20]. The Mg–3Al–1Zn alloy sheets with a tilted basal texture were obtained by asymmetric rolling and compared with a normal symmetrically rolled sheet, the ASR-processed sheet showed a larger uniform elongation. Therefore it is an effective means to enhance the room temperature formability of magnesium alloy sheets by weakening the basal texture.

In previous researches [21], a method that we had termed 'repeated unidirectional bending' (RUB) could effectively improve the (0 0 0 2) basal texture of magnesium alloy sheets. In this study, the RUB had been used to change the textural components of cold-rolled magnesium alloy sheet. The through-thickness texture gradient was systematically investigated during RUB and annealing by EBSD measure and the effect of texture on mechanical properties was discussed. This method not only improves the mechanical properties by improving the basal texture but also enriches the

* Corresponding author at: National Engineering Research Centre for Magnesium Alloys, College of Materials Science and Engineering, Chongqing University, Chongqing 400044, PR China. Tel.: +86 23 65112239; fax: +86 23 65102821.
E-mail address: gshuang@cqu.edu.cn (G. Huang).

0925-8388/$ – see front matter © 2009 Elsevier B.V. All rights reserved.
doi:10.1016/j.jallcom.2009.09.090

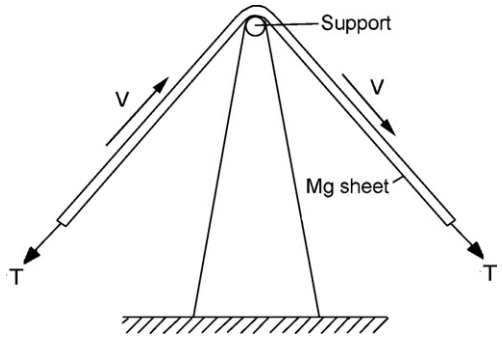

Fig. 1. Schematic illustration of apparatus for RUB.

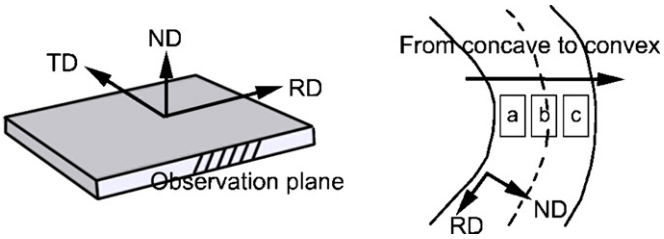

Fig. 2. Sketch maps of the orientation of the specimens for scanning electron microscopy. (a) Observation plane. (b) Measurement positions for EBSD analysis in the RD–ND plane of the RUB-processed sheets. Position a is near the concave side, b in the centre and c near the convex side.

research methods of magnesium alloy sheet property improvements.

2. Experimental procedures

Commercial AZ31B magnesium alloy (Mg–3 wt.% Al–1 wt.% Zn) sheets with a thickness of 0.8 mm, cut into 800 mm × 200 mm (length × width) pieces, were used in the experiments. Fig. 1 shows an abridged general view of the RUB process, where the magnesium alloy sheets were bent on a cylindrical support under a constant force T with a constant speed v. The bend direction was parallel to RD direction of sheet; in other word: the sheets were bent at a constant speed v along the RD. The radius of the cylindrical support was 1 mm and the bending angle was 90°. In the experiments, six-pass bending was used. Before RUB was performed, part of a magnesium alloy sheet was machined away to serve as an as-received specimen. All of the specimens used in the experiments were from the central portions of sheets. Part of the specimens that had undergone RUB was then annealed at 260 °C for 1 h.

The microstructure was observed by using a metallographic microscope and the macroscopic texture was obtained by X-ray. The X-ray texture analysis was performed for acquiring (0 0 0 2) pole figure using an X-ray diffractometer (XRD, Rigaku DMAX-1400 model) with Cu Kα radiation, a voltage of 40 kV and a current of 100 mA. From the normalized and corrected data, the pole figures were constructed. The surface of sheet was used as observation plane of texture. For the sheets underwent RUB, the observation planes of texture by XRD were the convexes. Electron backscatter diffraction (EBSD) experiments were conducted using a longitudinal section, which was selected as the observation plane as shown in Fig. 2(a). The EBSD analysis was performed at three places through the thickness of the sheet, as shown in Fig. 2(b). The as-received sheets, processed by large-deformation cold rolling and recrystallization annealing, had a uniform microstructure. So, in the case of the as-received specimen, the zone used in the scanning electron microscope for EBSD analysis could be any one of the zones a (near the concave side), b (in the centre of the thickness) or c (near the convex side) shown in Fig. 2(b); here, we used b as the scanning zone. However, for the other two specimens that were studied (processed by RUB and processed by RUB and annealed at 260 °C), all three of these zones were used as scanning zones, because of the different stress states that existed through the thickness from the concave to the convex side. An Oxford Instruments HKL system was used in the EBSD experiments. Scanning area of every zone is 300 μm × 100 μm (RD × ND), and the scanning step is 1 μm.

The mechanical properties of the magnesium alloy sheets in the three states described above were investigated by tensile testing. The tensile tests were carried out at the angles of 0° (RD), 45° and 90° (TD) between the tensile direction and the RD for investigating the anisotropy of the tensile properties, and the tensile strength, the 0.2% proof stress and the elongation were obtained as the average values of triplicate tests in each tensile direction.

3. Results and analysis

3.1. 3.1Microstructure and texture evolution

The through-thickness amount of strain was estimated using curvature radius during RUB. First, we assume that the center line of sheet-thickness have not elongation or contraction in length during bending and the frictional force between the concave side and the support is not considered. Under pure moment, the part of the inside of the center line becomes short due to compression and the part of the outside of the center line becomes long due to tension. Thus the deformation amount of the unit length can be expressed during bending:

$$e = \frac{R - R_n}{R_n} \quad (1)$$

where e is the bending strain, R is the radius of curvature, and R_n is the radius of neutral layer. For RUB, the bending radius 1 mm and the thickness of sheet is 0.8 mm, thus the deformation amount of the sheet-surface can achieve to about 28% during a pass RUB. In this conclusion, the deformation amount does not take into account the unbending deformation after passing the support. During the following passes, the deformation amount was superposed.

Fig. 3 shows the microstructures of the different magnesium alloy sheets. For the as-received sheet, the grains were fine. After the RUB was carried out at room temperature, some twins were found. Fig. 4 showing an EBSD mapping by orientation-imaging microscopy (OIM) and the misorientation angle distribution of the specimen undergoing RUB exhibited obvious increasing the number of grain boundaries near 86°. These grain boundaries may originate from $\{1\,0\,\bar{1}\,2\}$ pyramidal twins formed during bending because basal planes in twinned and untwined region from an angle 86.3° [22,23]. And these twins mainly existed in the grains with the Schmid factor of about 0.1–0.3. After the magnesium alloy sheet underwent RUB was annealed at 260 °C, the twins disappeared owing to static recrystallization and the grains near the surface of sheet grew obviously. This is because the magnesium alloy sheets used in the experiments have a given thickness. Thus there is a gradient of strain during bending of a sheet. The amount of defor-

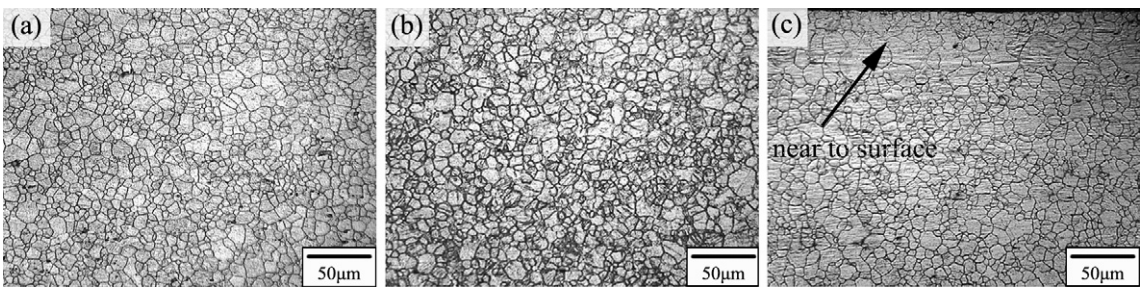

Fig. 3. Optical micrographs of (a) as-received sheet, (b) RUB without annealing sheet and (c) RUB + 260 °C annealing sheet.

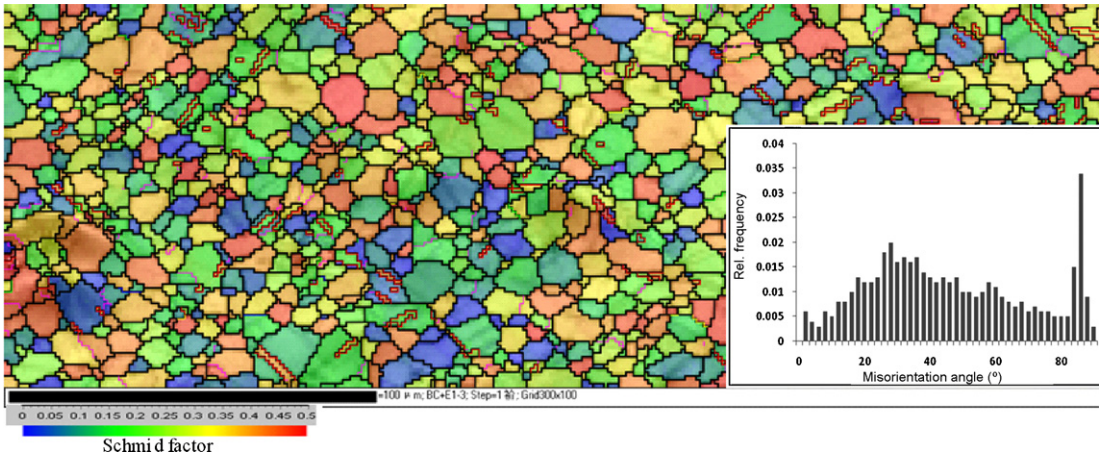

Fig. 4. Orientation map and distribution of misorientation angle in the specimen undergoing RUB. Here, red lines mark the $\{1\ 0\ \bar{1}\ 2\}$ twinning boundaries. Colours corresponding to different levels of basal Schmid factors are shown in bottom, when the tensile stress is applied in the RD. (For interpretation of the references to color in this figure legend, the reader is referred to the web version of the article.)

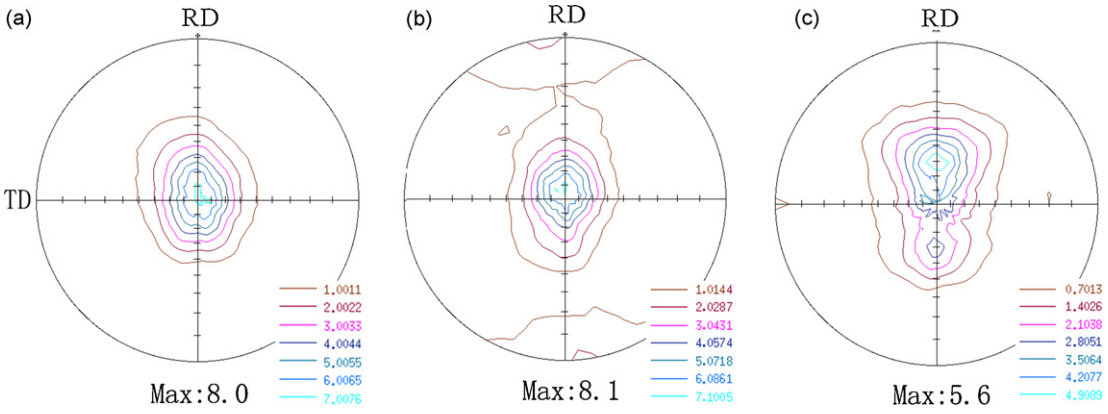

Fig. 5. {0 0 0 2} pole figures of the magnesium alloy sheets (a) as-received sheet, (b) RUB without annealing, (c) RUB + 260 °C annealing.

mation experienced by the region near the surface is higher than that in the center, which makes it possible to produce the gradient microstructure with the coarse-grained surface layer and the fine-grained layer in the middle of the sheet [24].

The XRD basal pole figures of the magnesium alloy sheets with different states are shown in Fig. 5. The strong basal texture existed in as-received magnesium alloy sheet (Fig. 5(a)). For the magnesium alloy sheet underwent RUB, the *c*-axes of the grains had a more

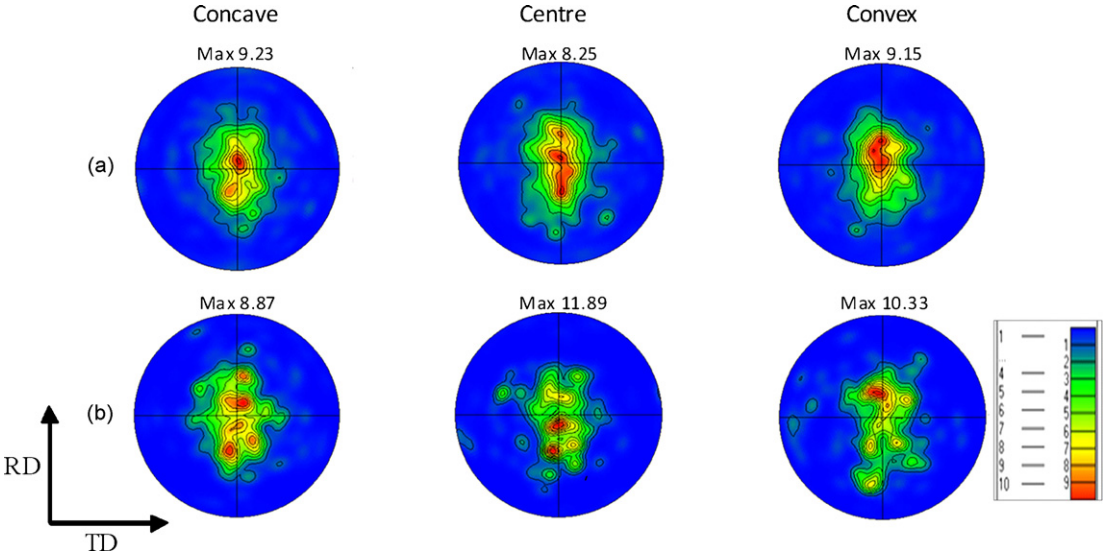

Fig. 6. {0 0 0 2} pole figures of specimens after (a) RUB without annealing, (b) RUB + 260 °C annealing. 'Concave', 'centre' and 'convex' represent the areas a, b and c, respectively, as shown in Fig. 2(b).

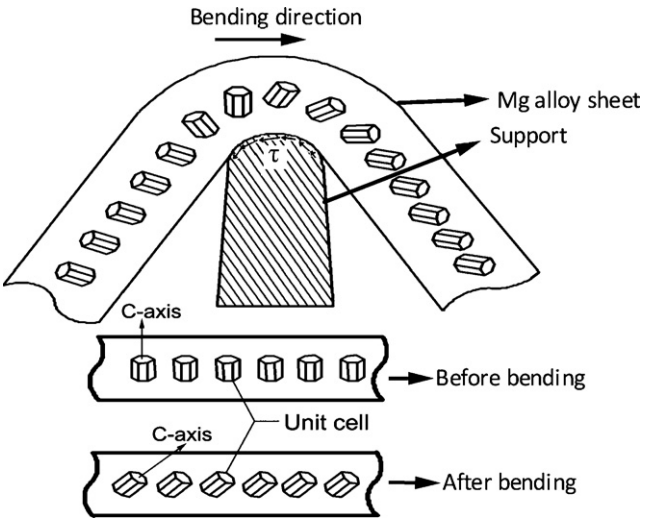

Fig. 7. Schematic diagram of grain rotation during RUB.

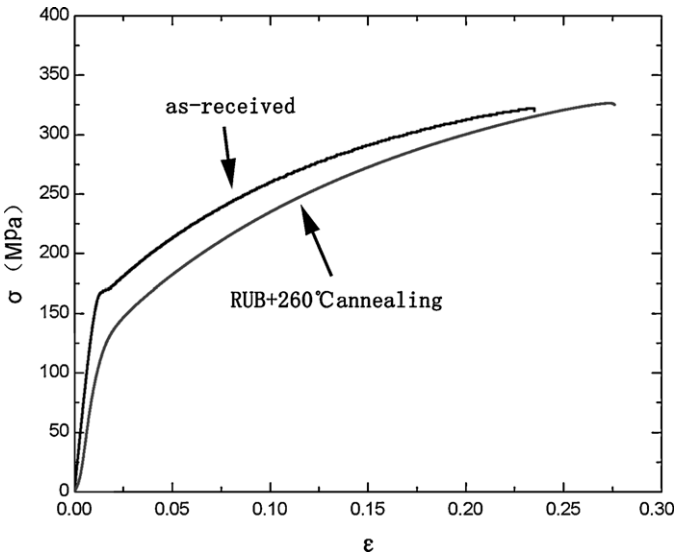

Fig. 9. True stress–strain curves of the as-received sheet and the RUB + 260 °C annealing sheet in the tensile directions of RD.

spread distribution in the RD and the basal texture tended to incline from the ND towards the RD. After the magnesium alloy sheet underwent RUB was annealed at 260 °C for 1 h, texture components became more disperse with appearing more pole peaks, and the basal texture were weakened because *c*-axis becomes inclined from the ND towards the RD. However, the *c*-axis is mainly distributed near directions parallel to the RD. This indicates that a close relationship exists between the recrystallization texture and the grain orientation of the deformed matrix.

For RUB, at the beginning stage of the bending, when the sheet passes over the support, it is very difficult to activate basal slip during bending because of the strong basal texture. At this stage, plastic deformation depends mainly on prismatic slip and pyramidal twins. The result of prismatic slip is that the grains rotate around the *c*-axis, but the basal-plane orientation does not change. However, pyramidal twins cause the basal planes of the grains to rotate to an orientation that forms an angle with the untwined region [25]. During the following passes, the orientations and stress states of the grains are changed because of the alternating operations of slip and twinning. With an increase in the basal Schmid factor and activation of the basal slip system, an angle is formed between the basal planes of the grains and the bending direction so that the *c*-axis becomes inclined from the ND towards the RD.

The EBSD technology was used to discuss the through-thickness texture gradient of magnesium alloy sheets underwent RUB. The basal pole figures of the specimen that underwent RUB without annealing are shown in Fig. 6(a). For the concave and the convex sides, the *c*-axis was inclined by 0–20° from the ND towards the RD. The authors' opinion is that the *c*-axes of the grains can rotate towards the bending direction during RUB, as shown in Fig. 7, which shows a schematic diagram of the grain rotation during bending and also the frictional force between the concave side and the support. Of course, this conclusion needs to be further researched. The texture orientation of the concave side is more concentrated in a region where the *c*-axis is inclined from the ND towards the RD by about 15°. This is partly because the concave side of the sheet was subject to an additional shear deformation, which was induced mainly by the friction between the sheet and the support during RUB [13,14]. With regards to the centre portion of the sheet-thickness, this cannot be considered as a neutral layer where the degree of deformation was at its smallest, and it certainly cannot be considered as a layer with no deformation, because the difference between the compressive yield strength and tensile yield strength of magnesium alloys leads to a shift of the neutral layer during bending, and the range of the neutral layer needs to be determined. Thus the centre portion of the thickness can be considered only as an interior portion of the sheet and is expected to have a complex stress state. For these reasons, the texture distribution of the centre portion was different from that of both surfaces and evolved into an elongated shape around the ND with the elongation direction

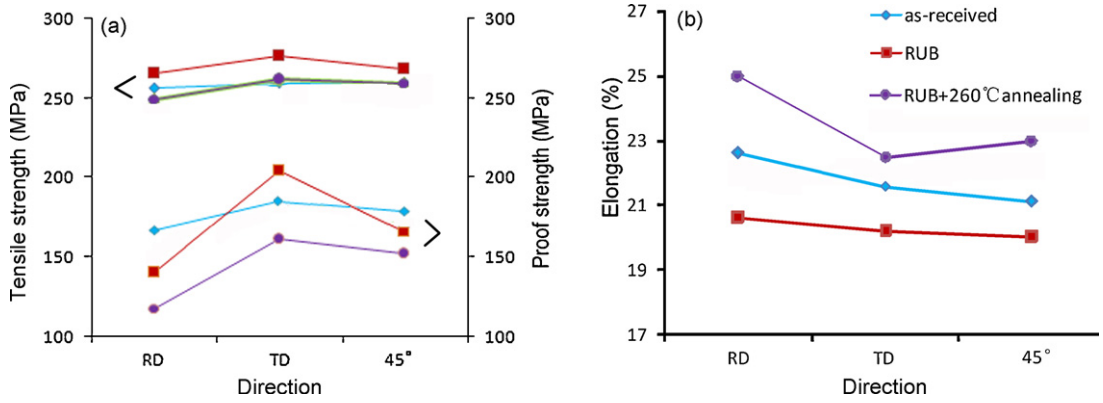

Fig. 8. (a) Ultimate tensile strength and 0.2% proof strength; (b) fracture elongation of the as-received sheet and the RUB-processed sheets in the tensile directions RD, TD and 45°.

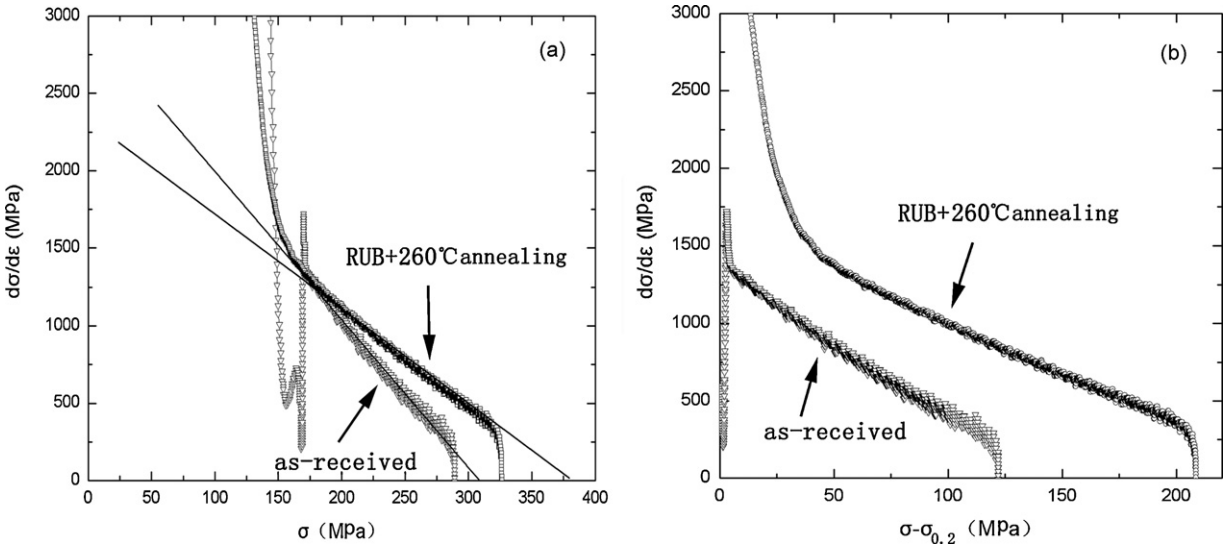

Fig. 10. Work-hardening rates of the as-received sheet and the RUB + 260 °C annealing sheet during the tensile deformation in the RD as a function of (a) σ and (b) $\sigma - \sigma_{0.2}$.

parallel to the RD. This indicated that the basal texture was maintained near the neutral layer. Fig. 6(b) shows the pole figures of the specimen that underwent RUB followed by annealing at 260 °C. The basal texture is weakened and the pyramidal components of the texture are increased significantly. The texture components have become more dispersed, especially on the concave and the convex sides, and the basal texture has been weakened significantly. However the texture orientation of the centre portion appears to be relatively concentrated near the basal texture. These results also indicate that it is easier for nuclei in high-deformation regions to grow spontaneously, and that the less deformed grains disappeared during static recrystallization. A model [26] for the simulation of deformation and recrystallization textures in close-packed hexagonal metals can also be used to explain the texture evolution during recrystallization annealing. The experimental results and the predictions of the model were consistent when nucleation took place in the grains with the highest stored plastic energy. In our study, the experimental evidence indicates that during recrystallization annealing the less deformed grain orientations disappear such as basal texture, which means that the more deformed grains nucleate and consume the less deformed ones.

3.2. Mechanical properties

The differences in the mechanical properties of the sheets in the three states studied, shown in Fig. 8, can be attributed mainly to the effects of texture and microstructure because the sheets in the three states had approximately the same average grain size, which was about 7 μm as determined by EBSD.

The tensile strength, 0.2% proof strength and fracture elongation are shown in Fig. 8. The tensile strength did not show any obvious change with the tensile orientation of the specimens. This indicated that the texture had a weak effect on the tensile strength [14]. The tensile strength of the sheets that underwent RUB without annealing was slightly larger than that of the other specimens because of work hardening. Some studies [27,28] have found that twinning induced during RUB can induce work hardening. For the sheet that underwent RUB without annealing, the 0.2% proof strength was lower in the RD and 45° tensile orientations than in the TD tensile orientation. These results indicated that RUB induced the *c*-axis to rotate towards the RD and lowered the proof strength. But the fracture elongations of the sheet that underwent RUB without annealing were lower in all tensile orientations than the values for the other sheets owing to work hardening; some researches [29,30] have suggested that deformation twinning is harmful for the forming of sheets. However, for the sheet that underwent RUB followed by annealing at 260 °C, the 0.2% proof strength, which showed a large decrease of about 10–50 MPa in all tensile orientations, was much lower than the values for the other sheets. Further, the fracture elongation of the sheet that underwent RUB followed by annealing at 260 °C was improved in all tensile orientations owing to the elimination of work hardening and twins. Because the *c*-axis was mainly inclined towards the RD, the proof strength was lowest and the fracture elongation showed the largest increase in the RD tensile orientation.

3.3. Influence of texture on work hardening and ductility at room temperature

The true stress–strain curves of the as-received sheet and the sheet underwent RUB followed by annealing at 260 °C in the tensile directions of RD are shown in Fig. 9. Compared with the as-received sheet, the strain hardening effect was stronger for the sheet underwent RUB followed by annealing at 260 °C after the macroscopic yielding. Fig. 10 shows macroscopic work-hardening rates ($d\sigma/d\varepsilon$) of the as-received sheet and the sheet underwent RUB followed by annealing at 260 °C under the tensile deformation in the RD as the functions of σ and $\sigma - \sigma_{0.2}$, where σ, $\sigma_{0.2}$ and ε are true stress, proof stress and true strain, respectively. The $\sigma - \sigma_{0.2}$ is related to the dislocation contribution to the flow stress [31]. As-received sheet shows first a steep hardening decrease in Fig. 10(a), due to a short elastoplastic transition. When the true stresses were about 150–170 MPa, the hardening rate was very low for as-received sheet. The result indicated an obvious yield point existed in as-received sheet. When the true stresses were above 175 MPa, the work-hardening rates decreased linearly with increasing the stress for both sheets and a smaller slope was observed for the sheet underwent RUB followed by annealing at 260 °C. Similar conclusions were obtained in Fig. 10(b). After the elastic–plastic transition, the decrease of work hardening may be related to soft behavior of the dynamic recovery originating from cross-slip of ⟨*a*⟩ dislocations from basal to prismatic planes [31]. For the sheet underwent RUB followed by annealing at 260 °C with a tilt basal texture, the slower slope indicated that the prismatic ⟨*a*⟩ slip was depressed owing to the activation of basal slip. For the magnesium alloy with the inclined basal texture, it

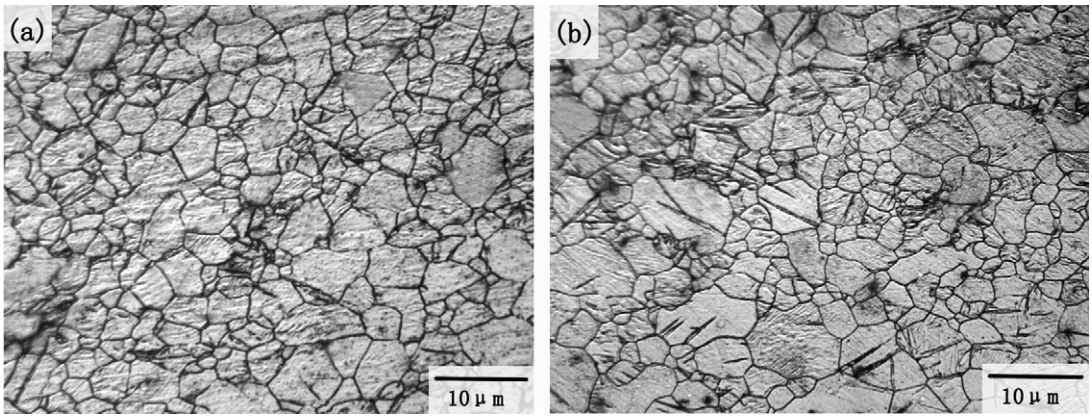

Fig. 11. Microstructures of the tensile specimens after 10% permanent straining in the RD of (a) the as-received sheet and (b) the RUB + 260 °C annealing sheet.

was easier to activate the $\{1\,0\,\bar{1}\,2\}$ twin at the early stage of tensile deformation [12]. Fig. 11 shows the microstructure results of the tensile specimens after 10% permanent straining in the RD of the as-received sheet and the sheet underwent RUB followed by annealing at 260 °C. The fraction of twins in the sheet underwent RUB followed by annealing at 260 °C was larger obviously than that of as-received sheet. At the beginning of plastic deformation, the formation of $\{1\,0\,\bar{1}\,2\}$ twin can relax the stress concentration and accommodate the strain incompatible owing to dislocation $\langle a\rangle$ slip [32]. Further the twin boundaries can also act as barriers to dislocation motion and becomes a source of work hardening. Therefore the dynamic recovery tended to be depressed due to the limited non-basal slips, and a higher work hardening was maintained. In recently, some researches [33,34] have reported that $\{1\,0\,\bar{1}\,2\}$ twinning, which gives extension along the *c*-axis in magnesium and its alloys, appears to increase the uniform elongation and decrease the proof strength seen in tensile tests. Ref. [35] indicated the improvement of elongation and described that this texture provided the favored orientation for $\{1\,0\,\bar{1}\,2\}$ extension twinning, which induced the increase in work hardening and in turn led to a larger uniform elongation. Ref. [31] thought that the hardening rate controls the ductility in magnesium alloy at room temperature. Therefore, the larger elongation of the sheet underwent RUB followed by annealing at 260 °C can be attributed to the higher work hardening, which was originated from the combination of the depressed dynamic recovery and the twin-induced work hardening.

4. Conclusions

In summary, the evolution of the texture of AZ31B magnesium alloy sheets during RUB and annealing has been investigated, and the mechanical properties of the RUB-processed sheets, with an inclination of the *c*-axis towards the RD, were compared with those of the as-received magnesium alloy sheets. After RUB, the proof strength of the sheets, whose grain orientations mostly had an inclination of the *c*-axis of towards the RD, was lowered in the RD and 45° tensile orientations. However, the fracture elongation was very low owing to work hardening. After RUB and annealing at 260 °C for an hour, the texture components became more dispersed along directions parallel to the RD. Further, the fracture elongation was considerably increased, especially in the RD, and the proof strength was lowered in all tensile orientations. The larger elongation of the sheet underwent RUB followed by annealing at 260 °C can be attributed to the higher work hardening. These results indicate that RUB processing is an effective way of improving the mechanical properties of magnesium alloy sheets at room temperature by controlling the texture.

Acknowledgements

This work was supported by the National Natural Science Foundation of China under Grant No. 50504019, Natural Science Foundation of CQ CSCT under Grant No. 2008BB4040 and Scientific and Technological Project of CQ CSCT under Grant No. 2008AA4028. Additionally, the authors would like to thank Professor Wenhai Ye for the texture analysis.

References

[1] M.M. Avedesian, H. Baker, ASM Int. 274 (1999).
[2] H. Yoshinaga, R. Horiuchi, Trans. JIM 5 (1963) 14.
[3] S. Suwas, G. Gottstein, R. Kumar, Mater. Sci. Eng. A 471 (2007) 1–14.
[4] K. Máthis, J. Gubicza, N.H. Nam, J. Alloys Compd. 394 (2005) 194–199.
[5] L. Jin, D.L. Lin, D.L. Mao, X.Q. Zeng, W.J. Ding, J. Alloys Compd. 426 (2006) 148–154.
[6] W.M. Gan, M.Y. Zheng, H. Chang, X.J. Wang, X.G. Qiao, K. Wu, B. Schwebke, H.-G. Brokmeier, J. Alloys Compd. 470 (2009) 256–262.
[7] J.B. Lin, Q.D. Wang, L.M. Peng, H.J. Roven, J. Alloys Compd. 476 (2009) 441–445.
[8] Y.J. Chen, Q.D. Wang, H.J. Roven, M.P. Liu, M. Karlsen, Y.D. Yu, J. Hjelen, Scripta Mater. 58 (2008) 311–314.
[9] Y.J. Chen, Q.D. Wang, H.J. Roven, M. Karlsen, Y.D. Yu, M.P. Liu, J. Hjelen, J. Alloys Compd. 462 (2008) 192–200.
[10] J.A. del Valle, M.T. Pérez-Prado, O.A. Ruano, Mater. Sci. Eng. A 410–411 (2005) 353–357.
[11] M.Y. Zhan, Y.Y. Li, W.P. Chen, Trans. Nonferrous. Met. Soc. China 18 (2008) 309–314.
[12] X.S. Huang, K. Suzuki, A. Watazu, I. Shigematsu, N. Saito, Mater. Sci. Eng. A 488 (2008) 214–220.
[13] G.S. Rao, Y.V.R.K. Prasad, Metall. Trans. 13A (1982) 2219–2226.
[14] X.S. Huang, K. Suzuki, A. Watazu, I. Shigematsu, N. Saito, J. Alloys Compd. 457 (2008) 408–412.
[15] X.S. Huang, K. Suzuki, A. Watazu, I. Shigematsu, N. Saito, J. Alloys Compd. 470 (2009) 263–268.
[16] X.S. Huang, K. Suzuki, A. Watazu, I. Shigematsu, N. Saito, J. Alloys Compd. 479 (2009) 726–731.
[17] X.S. Huang, A. Suzuki, N. Saito, Mater. Sci. Eng. A 508 (2009) 226–233.
[18] W.J. Xia, Z.H. Chen, D. Chen, S.Q. Zhu, J. Mater. Process. Technol. 209 (2009) 26–31.
[19] W.J. Kim, J.D. Park, W.Y. Kim, J. Alloys Compd. 460 (2008) 289–293.
[20] S.-H. Kim, B.-S. You, C.D. Yim, Y.-M. Seo, Mater. Lett. 59 (2005) 3876–3880.
[21] G.S. Huang, W. Xu, G.J. Huang, H.C. Li, F.S. Pan, Mater. Sci. Forum. 610–613 (2009) 737–741.
[22] A. Jäger, P. Lukáč, V. Gärtnerová, J. Haloda, M. Dopita, Mater. Sci. Eng. A 432 (2006) 20–25.
[23] M.T. Pérez-Prado, J.A. del Valle, O.A. Ruano, Scripta Mater. 50 (2004) 667–671.
[24] Y. Takayama, J.A. Szpunar, H.T. Jeong, Mater. Trans. 42 (2001) 2050.
[25] Y. Yoshida, L. Cisar, S. Kamado, J.-I. Koike, Y. Kojima, Mater. Sci. Forum. 419–422 (2003) 533–538.
[26] D.E. Solas, C.N. Tomé, O. Engler, H.R. Wenk, Acta Mater. 49 (2001) 3791–3801.
[27] M.R. Barnett, Z. Kehavarz, A.G. Beer, D. Atwell, Acta Mater. 52 (2004) 5093–5103.
[28] A. Ayman, Salem, R. Surya, Kalidindi, D. Roger, Doherty, Acta Mater. 51 (2003) 4225–4237.
[29] S.M. Yin, F. Yang, X.M. Yang, S.D. Wu, S.X. Li, G.Y. Li, Mater. Sci. Eng. A 494 (2008) 397–400.

[30] J.W. Christian, S. Mahajan, Deformation twinning, Prog. Mater. Sci. 39 (1995) 131–150 (Great Britain).
[31] J.A. del Valle, F. Carreno, O.A. Ruano, Acta Mater. 54 (2006) 4247–4259.
[32] J. Koike, Metall. Mater. Trans. 36A (2005) 1689–1696.
[33] M.R. Barnett, Mater. Sci. Eng. A 464 (2007) 1–7.
[34] Y.N. Wang, J.C. Huang, Acta Mater. 55 (2007) 897–905.
[35] J. Bohlen, M.R. Nurnberg, J.W. Senn, D. Letzig, A.R. Agnew, Acta Mater. 55 (2007) 2101–2122.